Magnetic quantum phase transition in MnSi under hydrostatic pressure

C. Pfleiderer,* G. J. McMullan, S. R. Julian, and G. G. Lonzarich
Cavendish Laboratory and the Interdisciplinary Research Centre for Superconductivity, Madingley Road, Cambridge CB3 0HE, United Kingdom
(Received 6 November 1996)

The crossover from a spin-polarized to nonpolarized state as a function of pressure (p) at low temperature (T) has been investigated in MnSi via high-precision measurements of the electrical resistivity ρ and magnetic susceptibility χ. In the magnetic phase ($p<p_c\simeq 14.6$ kbar), $\rho\propto T^2$ at low T as expected for a Fermi liquid in a weakly polarized state. In the nonmagnetic phase ($p>p_c$), ρ vs T is consistent with the predictions for a marginal Fermi liquid model in which nearly critical spin fluctuations of long wavelength lead to a singular quasiparticle interaction. The transition is second order for $p<p^*\simeq 12$ kbar and weakly *first* order in the range $p^*<p<p_c$, where the transition temperature T_c lies below a peak of χ vs T. The variation of T_c with p and of both ρ and χ with T and p may be understood in terms of a model of quantum critical phenomena. [S0163-1829(97)04213-6]

I. INTRODUCTION

In the Landau model of a normal Fermi liquid, fermion quasiparticles are regarded, in general, as interacting entities, but the scattering on the Fermi surface at absolute zero is assumed to be ''nondiffractive.''[1] The assumption of scattering processes at $T=0$, which involve particle exchanges but no other momentum transfer, can clearly break down when the residual interaction has an attractive component. In this case, quasiparticles may form bound states and condense into superconducting or magnetically ordered phases. There is, however, another way in which the normal description can fail. The suppression of real scattering processes by the Pauli principle is based on the premise that the quasiparticle interaction is both repulsive and nonsingular for transitions near the Fermi surface. This latter postulate is not satisfied, for instance, for the case of the Lorentz magnetic force between moving charges.[2] Though the effects of the Lorentz magnetic force may become shielded at long range for a many-body system, the residual quasiparticle interaction produced by this magnetic coupling is expected to remain long range. It can hence lead to a cross section for quasiparticle scattering which is singular for small momentum transfers at the Fermi level. An analogous contribution, but of much greater strength and potential importance, arises from an effective coupling associated with a molecular exchange field produced by quasiparticles in a medium on the verge of a continuous magnetic phase transition. The range of this interaction may be measured in terms of the magnetic correlation length which diverges as the magnetic critical point T_c is approached. Thus, in systems of reduced dimensionality in which T_c tends to be automatically suppressed by enhanced fluctuations of the order parameter or in three-dimensional materials in which T_c is quenched by means of some control parameter, such as hydrostatic pressure (p), the Fermi liquid description, in its familiar form, may break down.[1,3]

In this paper we consider the *d* transition metal MnSi, in which the relevant exchange field, capable of producing a long-range interaction between fermionic quasiparticles, is associated with overdamped spin fluctuations. The nearly critical magnetic fluctuations in MnSi, which have been extensively studied experimentally[4] and theoretically,[5,6] are essentially of long wavelength. This together with a weak spin-orbit coupling and a cubic crystal structure ($B20$) suggests that the important components of the spin fluctuations might be described in a first approximation in terms of an isotropic homogeneous model. This model is equivalent, in details most relevant to our discussion, to that employed in cases in which transverse currents associated with gauge fields[2,8,9] (rather than critical spin fluctuations of interest here) are important.

At ambient pressure in zero magnetic field and below $T_c\sim 30$ K, MnSi appears ferromagnetically aligned over distances shorter than the wavelength ($2\pi/Q\simeq 190$ Å) of a gradual, weakly temperature and pressure-dependent, helical modulation.[4,10] The magnitude of T_c is far below that expected from conventional band theory[11] but consistent, as are other low-temperature thermal properties, with the predictions of a model in which the nonlinear effects of spin fluctuations are treated in a self-consistent rotationally invariant Hartree approximation.[6,12] It is found that T_c falls monotonically with increasing pressure p and tends to zero at $p_c=14.6$ kbar,[13,14] the critical pressure of a magnetic quantum phase transition.

II. EXPERIMENTAL TECHNIQUES

The nature of the low-temperature state of MnSi near p_c was investigated via measurements of the electrical resistivity ρ and magnetic susceptibility χ in pressure and temperature ranges extending up to 18 kbar and down to 20 mK, respectively. A number of single crystals[11,15] with different residual resistivity ratios [$\mathrm{RRR}=\rho(293\ \mathrm{K})/\rho(T\rightarrow 0\ \mathrm{K})$] were studied. Except when otherwise indicated the results presented below were obtained using a specimen from the sample with the highest RRR (≈ 243) that had previously been used in a de Haas–van Alphen investigation.[11] From the observed scattering or Dingle temperature the carrier mean free path in this sample was estimated to be 3000 Å.

Pressures were generated in a conventional piston-cylinder clamp cell with a BeCu outer and maraging steel inner sleeve. An equal volume mixture of iso- and *n*-pentane, which remains liquid at room temperature over the range of pressures explored, was used as the pressure-transmitting medium. The pressure was inferred from the resistivity of a calibrated manganin coil at room temperature and from the superconducting transition of Sn at low temperature. A calibration of our cell with the above transmitting medium shows that the pressure of the cell is essentially temperature independent below ≈ 120 K, i.e., in the range of interest in this study.[16] The temperature was measured with calibrated Ge and carbon-glass resistors as well as a GaAs diode. The sensors were all heat sunk to a Cu enclosure tightly fitted around the pressure cell. Electrical and additional thermal contact was achieved with Cu wires heat sunk on the Cu enclosure and soldered to the sample via the eutectic alloy $Au_{0.8}Sn_{0.2}$. To maintain adequate pressure and temperature homogeneity, the cell was precooled slowly (below 0.3 K/min) and measurements at low temperature carried out with sweep rates below 20 mK/min. Under these conditions no evidence for inhomogeneities in warming and cooling cycles was observed in either the Sn transition or in measurements of the resistivity and susceptibility of MnSi. In particular, the width of the Sn transition as measured resistively or inductively (as part of the background signal in the susceptibility data) was found to be independent of pressure in our experimental range.[17] This enables us to measure relative changes in pressure to an accuracy of ± 0.02 kbar. The reproducibility in cooling and warming cycles coupled with the consistency among the various calibrated manometers suggests that our temperature accuracy is better than ± 5 mK below 10 K and typically ± 30 mK at higher temperatures.

The resistivity was measured via a conventional four-terminal ac-phase-sensitive technique. The differential susceptibility was investigated by a field modulation method based on a drive coil and a carefully balanced pair of pickup coils, all mounted within the actual pressure cell.[17] For measurements of ρ the current density was typically $10^3 \mathrm{A/m}^2$ at 1.5 Hz and for measurements of χ a modulation field of 2×10^{-4} T at 23 Hz was used. Under these conditions, effects of sample heating and spurious background voltages could be ignored. In all cases the current and modulation field were directed along the $\langle 100 \rangle$ axis of the crystalline sample.

Empty coil measurements show that the ac susceptibility background voltage in the experimental pressure range is essentially temperature independent below 120 K. The susceptibility data were corrected for this temperature independent background as well as for a small pressure-related change in sensitivity. The corrected data were scaled assuming a negligible pressure variation of the slope of χ^{-1} vs T above 40 K. This procedure is consistent to an accuracy of $\pm 5\%$ with the results of more recent measurements.[18] The absolute value of the slope of χ^{-1} vs T above 40 K, measured with a superconducting quantum interference device (SQUID) magnetometer at ambient pressure, was found to be consistent with that previously reported in lower-quality samples. In the paramagnetic state the imaginary component of the low-frequency ac susceptibility was in all cases below our detection limit. A non-negligible imaginary component, attributed to low-frequency dissipative effects of magnetic domains, was, however, observed in the magnetically ordered state.

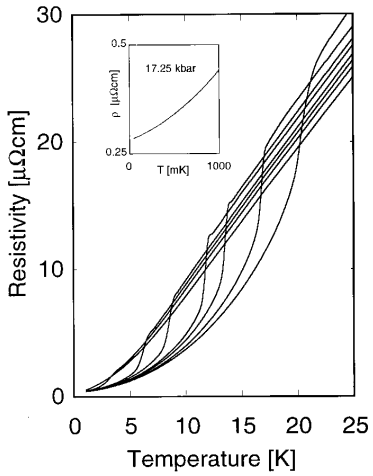

FIG. 1. The resistivity vs temperature at different pressures (5.55, 8.35, 10.40, 11.40, 12.90, 13.55, 14.30, and 15.50 kbar going down, starting from the top curve at the far right). The magnetic ordering temperature T_c (marked by the shoulder in ρ vs T) decreases towards absolute zero at $p_c \simeq 14.6$ kbar. For $p > p_c$ a non-Fermi-liquid form of ρ vs T (i.e., a variation T^β with $\beta < 2$) is seen to extend over several orders of magnitude down to mK temperatures (inset).

III. RESULTS

As shown in Fig. 1, the resistivity drops monotonically by approximately three orders of magnitude in all cases on cooling from 300 K to 20 mK. For pressures below $p_c \simeq 14.6$ kbar, a shoulder appears in ρ vs T, together with a single peak in $\partial\rho/\partial T$, marking the onset of magnetic order. The peak position, which we identify with the transition temperature T_c, is monotonically decreasing and appears to go towards zero continuously, but with a high slope at p_c. As shown in Fig. 2, the exponent α defined by the relation $T_c^\alpha \propto p$ is close to 2 near p_c but falls well below 2 for $p < p^* \simeq 12$ kbar. We note that the form of T_c vs p is not sensitive to the precise criterion used to identify T_c from the region of the peak in $\partial\rho/\partial T$ and is essentially the same as that inferred from the peak in χ vs T (see below and Fig. 2).

In the magnetic phase below p_c, ρ has a quadratic (T^2) temperature dependence for $T \ll T_c$. This is the behavior expected for a Fermi liquid in a paramagnetic or weakly polarized state. As p_c is approached, the T^2 regime collapses, while a quasilinear temperature variation of ρ above T_c is seen to extend to progressively lower temperatures (Fig. 1). Over the entire temperature range investigated the temperature variation of ρ above p_c is slower than quadratic. This departure of ρ vs T from the conventional Fermi liquid form is highlighted in Fig. 3 where $\Delta\rho/T^2$, in which $\Delta\rho = \rho - \rho_0$ and ρ_0 is the small residual value of ρ in the limit $T \to 0$ at each pressure (inset of Fig. 1), is plotted as a function of T. We stress that the small size of ρ_0 allows us to treat $\Delta\rho$ as an intrinsic property of the pure metallic state in the analysis of Sec. IV D. As shown in Fig. 3, $\Delta\rho/T^2$ saturates at low

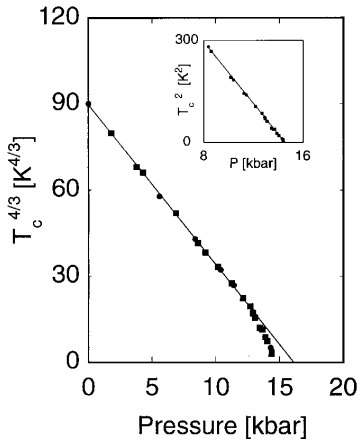

FIG. 2. The pressure dependence of the transition temperature inferred from the resistivity data (■) and the magnetic susceptibility data (●). For $p<p^*$ ($\simeq$12 kbar), $T_c^{4/3}$ is approximately linear in p, while for $p^*<p<p_c$ ($\simeq$14.6 kbar), T_c^2 is linear in p (inset).

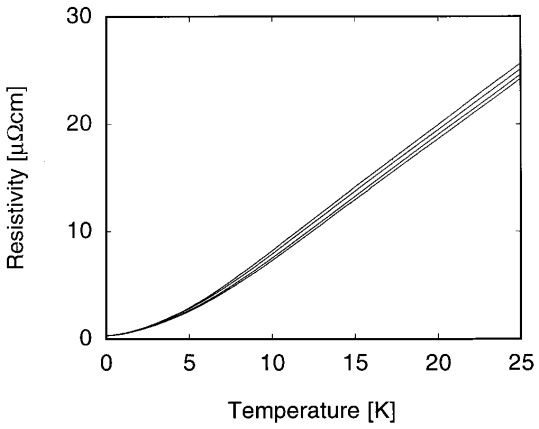

FIG. 4. The resistivity vs temperature at different pressures above p_c (14.75, 15.50, 16.60, and 17.20 kbar, starting from the top curve). The non-Fermi-liquid exponent β (inset of Fig. 3) remains unchanged in this pressure range).

T in the magnetic Fermi liquid state below p_c, but grows with decreasing temperatures without apparent limit in the paramagnetic state above p_c. Here the exponent β defined via $\Delta\rho\propto T^\beta$ is everywhere less than 2 and increases gradually from approximately 1.5 at 10 K to a maximum of 1.6 at the lowest temperatures reached (Figs. 3 and 4).

The singular behavior of $\Delta\rho/T^2$ is consistent with the anomalously strong *cross section* for quasiparticle-quasiparticle scattering and hence, as discussed in the Introduction, with the presence of a long-range component in the quasiparticle potential at low temperatures. (In analogy to the more elementary problem of fermions interacting via a short-range potential, we may think for $\Delta\rho/T^2$ as a measure of the cross section before account is taken of the T^2 factor arising from the Pauli principle constraint in the scattering.) A related divergence is anticipated for C/T, the ratio of the heat capacity to the temperature, the singular component of which represents the effect on the quasiparticle *mass* of the self-interaction associated with the long-range potential. In an intuitive interpretation of the results of the theoretical analysis presented in the following section, one may say that the *size* of the quasiparticles as measured either via an effective *cross section* ($\Delta\rho/T^2$) or an effective *mass* (C/T) tends to be singular near p_c in the low-temperature limit.

We next turn to our study of the uniform susceptibility χ (Figs. 5 and 6) which sheds more light on the nature of the magnetic transition and the limitations of the simple interpretation of $\Delta\rho$ given above. For $p<p^*$, χ^{-1} is approximately

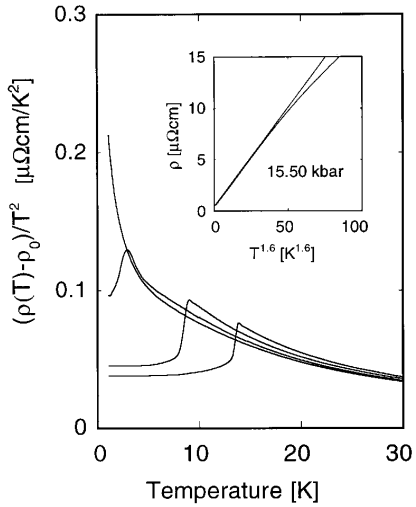

FIG. 3. The ratio of $\Delta\rho=\rho-\rho_0$ to T^2 vs temperature T at different pressures (10.40, 12.90, 14.30, and 15.50 kbar going up, starting from the bottom curve at the far left), highlighting the breakdown of the Fermi liquid form $\Delta\rho\propto T^2$ at low T as p_c is approached. Near p_c, $\Delta\rho\propto T^\beta$ with $\beta\simeq1.6$ in the low-temperature limit (curved line in the inset; the straight line above gives the asymptotic low temperature form).

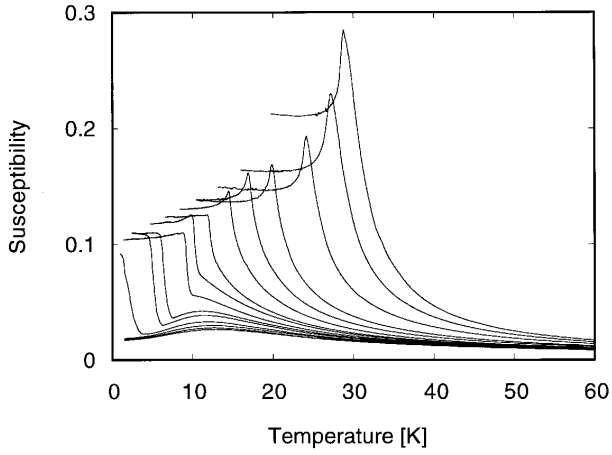

FIG. 5. The initial magnetic susceptibility (in SI units) vs temperature at different pressures (ambient, 1.80, 3.80, 6.90, 8.60, 10.15, 11.25, 12.15, 13.45, 13.90, 14.45, 15.20, 15.70, and 16.10 kbar going down, starting from the top curve at 30 K). For $p<p^*$ ($\simeq$12 kbar) χ exhibits a peak corresponding to a transition of *second* order, but for $p^*<p<p_c$ ($\simeq$14.6 kbar) the peak transforms into a step as expected for a transition of *first* order. The form of χ below the transitions is complicated by the effects of domains in the long-wavelength spin spiral state.

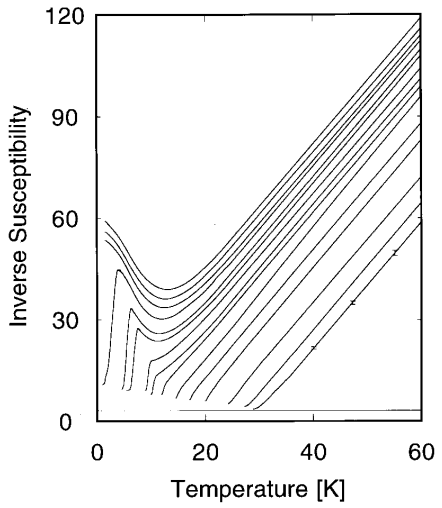

FIG. 6. The initial inverse magnetic susceptibility (in SI units) vs temperature at different pressures fitted from the data in Fig. 5 (at the same pressures, now going up, starting from the lowest curve). The error bars on the curve at ambient pressure indicate the noise level in the unfitted data. The small nonzero χ^{-1} at T_c arises from the effect of the long-wavelength helical modulation.

linear in temperature over a wide range. Moreover, it tends towards zero continuously at T_c as expected for a phase transition of *second* order. The behavior of χ^{-1} is more complex in the range $p^*<p<p_c$. The abrupt variation near T_c is reminiscent of a transition of *first* order. Although T_c in this regime collapses rapidly with increasing pressure, the transition width, as defined from the step in χ vs T, appears to remain constant. Moreover, this width increases with decreasing RRR and in a sample with a RRR of 80 the first-order regime is in fact not well defined (Fig. 7). This suggests that the transition width seen in Figs. 5 and 6 is probably neither intrinsic nor due to pressure inhomogeneities, but arises from residual defects in the sample.

Finally, we note that the value of T_c at the crossover from *second* to *first* order coincides roughly with the location of a minimum in χ^{-1} vs T in the paramagnetic phase. The initial fall of χ^{-1} vs T above p_c, and hence increase in magnetic response with temperature at low temperatures, appears to be an ubiquitous property of paramagnetic metals on the verge of magnetic order at low temperatures. This study provides us with an example of how this anomalous behavior of χ vs T changes in a pure metal in the vicinity of a magnetically ordered state.

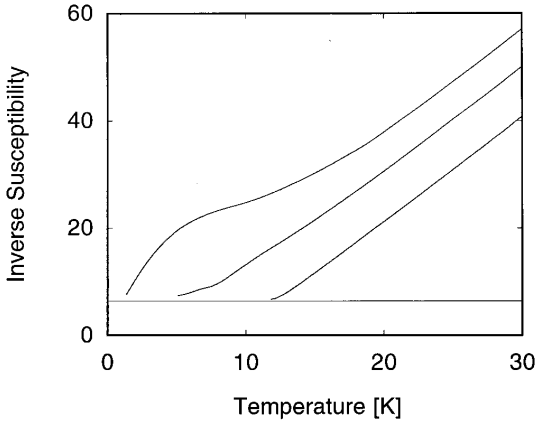

FIG. 7. As in Fig. 6, but for a sample with a residual resistivity ratio approximately 3 times smaller [at 10.60 kbar (below p^*), 13.20 kbar ($p^*<p<p_c$), and p_c, going up from the lowest curve]. The sharp first-order form of the transition seen in Fig. 6 near p_c is now replaced by a broad anomaly.

IV. THEORETICAL INTERPRETATION

A. Spin fluctuation spectrum

An interpretation of the T and p dependences of ρ and χ at low T might be sought within a framework of mutually interacting quasiparticles coupled via an effective long-range potential as discussed above. Equivalently, we may consider fermions coupled not to each other directly, but rather to a field (e.g., the electromagnetic field in the case of *bare* electrons) which effectively *mediates* the long-range interaction. We shall be concerned with a low-frequency long-wavelength description in which all fluctuations with wave vectors and frequencies above some cutoffs q_c and ω_c, respectively, have been effectively filtered out (i.e., all relevant field components outside of this window have been formally integrated out). In the end, the singular parts of the properties discussed below are found to be weakly dependent on such cutoffs.

For a system near a ferromagnetic instability at p_c, the important residual interaction field is the exchange molecular field. In the simplest approximation, a spatial Fourier component of this molecular field may be taken to be proportional to the corresponding Fourier component $\boldsymbol{m}_{\boldsymbol{q}}(t)$ of the space- and time-dependent magnetization $\boldsymbol{m}(\boldsymbol{r},t)$, associated with slow or nearly critical fluctuations. The focus of attention here is on the dynamical properties of $\boldsymbol{m}_{\boldsymbol{q}}(t)$ which, in the paramagnetic state, may be characterized by an appropriate relaxation spectrum $\Gamma_{\boldsymbol{q}}$. This relaxation spectrum together with the Bose function essentially defines the model described below for the dominant temperature dependences of the resistivity and heat capacity near the critical point in which $T_c \rightarrow 0$.

In a simple paramagnetic metal $\Gamma_{\boldsymbol{q}}$ is defined at low frequencies through the imaginary part for the wave vector $\boldsymbol{q}$ and frequency ω dependent susceptibility given by

$$\chi''_{\boldsymbol{q}\omega} = \omega \chi_{\boldsymbol{q}} \Gamma_{\boldsymbol{q}} / (w^2 + \Gamma_{\boldsymbol{q}}^2), \tag{4.1}$$

where $\chi_{\boldsymbol{q}}$ measures the strength of the low-ω component of the full, generalized susceptibility. In simple systems such as MnSi, which are of interest here, $\chi_{\boldsymbol{q}}$ will be assumed to reduce at low $\boldsymbol{q}$ to the wave-vector-dependent magnetic susceptibility. In the standard model,[5] supported by inelastic neutron scattering measurements in high-quality samples of a number of cubic, nearly ferromagnetic metals,[4,19] $\Gamma_{\boldsymbol{q}}$ is isotropic at low $q=|\boldsymbol{q}|$ and of the form

$$\Gamma_{\boldsymbol{q}} = \gamma_{\boldsymbol{q}} \chi_{\boldsymbol{q}}^{-1} = \gamma q^n (\chi^{-1} + c q^2), \tag{4.2}$$

in which γ and c are constants, χ is the temperature-dependent static susceptibility, and in the present case $n=1$ corresponding to the Landau damping in a homogeneous Fermi liquid. To discuss the role of $\Gamma_{\boldsymbol{q}}$ from a more general

point of view, it is helpful to introduce an exponent l such that $\Gamma_{\boldsymbol{q}} \propto q^l$ at low q. Well away from the critical region, χ^{-1} is finite and from Eq. (4.2) $l=n$. At the critical point $\chi^{-1} \rightarrow 0$, and provided that Eq. (4.2) continues to hold (see Sec. IV C), $l=n+2$. More generally at the critical point we assume $l=z$ where z is the dynamical exponent which, together with the spatial dimension d, enters the quantum description of critical phenomena.[3,20,21]

B. Population function

Both the resistivity and heat capacity of the system will depend on the amplitude of spontaneous thermal fluctuations of the molecular field or, essentially, of $\boldsymbol{m}_{\boldsymbol{q}}(t)$. Thus, we shall be interested in the thermal component $\langle |\boldsymbol{m}_{\boldsymbol{q}}|^2 \rangle_T$ of the variance of $\boldsymbol{m}_{\boldsymbol{q}}$, which is given by the fluctuation dissipation theorem as

$$\langle |\boldsymbol{m}_{\boldsymbol{q}}|^2 \rangle_T = \frac{6\hbar}{\pi} \int_0^{\omega_c} d\omega n_\omega \chi''_{q\omega}, \tag{4.3}$$

where $n_\omega = [\exp(\hbar\omega/k_B T) - 1]^{-1}$ is the Bose function. Equation (4.3) assumes a convention for the Fourier series of $\boldsymbol{m}$ in which $\langle |\boldsymbol{m}|^2 \rangle$ is simply the $\boldsymbol{q}$-space sum of $\langle |\boldsymbol{m}_{\boldsymbol{q}}|^2 \rangle$ per unit volume. Also note that for $k_B T \ll \hbar\omega_c$, a limit assumed throughout, the ω integral is effectively cut off by the Bose function so that the upper bound of the integral in Eq. (4.3) may be extended to infinity.

To simplify our discussion, it is useful to introduce a dimensionless population function $n_{\boldsymbol{q}}$ as shown in Ref. 3, which is defined as $\langle |\boldsymbol{m}_{\boldsymbol{q}}|^2 \rangle_T / (3\hbar\Gamma_{\boldsymbol{q}}\chi_{\boldsymbol{q}})$, and so from Eqs. (4.1)–(4.3)

$$n_{\boldsymbol{q}} \equiv \frac{\langle |\boldsymbol{m}_{\boldsymbol{q}}|^2 \rangle_T}{3\hbar\Gamma_{\boldsymbol{q}}\chi_{\boldsymbol{q}}} = \frac{2}{\pi} \int_0^\infty d\omega n_\omega \frac{\omega}{\omega^2 + \Gamma_{\boldsymbol{q}}^2} \equiv \eta(\hbar\Gamma_{\boldsymbol{q}}/k_B T), \tag{4.4}$$

where

$$\eta(x) = \frac{1}{\pi}\left[\ln\left(\frac{x}{2\pi}\right) - \frac{\pi}{x} - \Psi\left(\frac{x}{2\pi}\right)\right] \simeq \frac{1}{x(1+3x/\pi)} \tag{4.5}$$

and Ψ is the digamma function. The approximate and exact forms for η given in Eq. (4.5) differ by at most a few percent and are identical to leading order in both x and $1/x$. The low- and high-T limits of $n_{\boldsymbol{q}}$ are given by $(\pi/3)(k_B T/\hbar\Gamma_{\boldsymbol{q}})^2$ and $(k_B T/\hbar\Gamma_{\boldsymbol{q}})$, respectively. It is interesting to compare these limits with those of the corresponding population function for an undamped oscillator of frequency $\Omega_{\boldsymbol{q}}$, namely, the Bose function. In this case the high- and low-T limits are given by $(k_B T/\hbar\Omega_{\boldsymbol{q}})$ and $\exp(-\hbar\Omega_{\boldsymbol{q}}/k_B T)$, respectively. Note that whereas the high-T limits are similar, the low-T exponential freezing out of the population found in the undamped case is replaced by a more gradual quadratic temperature dependence for the overdamped modes described by Eq. (4.4). Normally, this T^2 dependence leads to the thermal energy, susceptibility, and resistivity, all being of the conventional Fermi liquid form. However, this need not be the case in low dimensions or near a critical point, where a rapid $\boldsymbol{q}$ dependence of $\Gamma_{\boldsymbol{q}}$ can lead to singular behavior from the low-$\boldsymbol{q}$ contribution to a sum over $\boldsymbol{q}$ of $n_{\boldsymbol{q}}$.

C. Non-Fermi-liquid exponents

In all the cases considered below the temperature dependence arises from a sum of the population function $n_{\boldsymbol{q}}$ as given in Eq. (4.4) weighted by a $\boldsymbol{q}$ factor of the form q^m. For generality, as discussed following Eq. (4.1), we set $\Gamma_{\boldsymbol{q}} \propto q^l$ so that in d dimensions

$$\sum_{\boldsymbol{q}} q^m n_{\boldsymbol{q}} \propto T^s \int_0^{x_c} dx \frac{x^{s-2}}{(1+x)}, \tag{4.6}$$

where $s \equiv (d+m)/l$, x_c is a cut off inversely proportional to T, and we have used the approximate form for η given in Eq. (4.5). If $s \leq 1$, the integral diverges at the lower bound and our model therefore breaks down. When $s>1$, Eq. (4.6) is finite and to leading order in T

$$\sum_{\boldsymbol{q}} q^m n_{\boldsymbol{q}} \propto \begin{cases} T^s, & 1<s<2, \\ T^2 \ln(T^*/T), & s=2, \\ T^2, & s>2, \end{cases} \tag{4.7}$$

where T^* is a constant. A crossover occurs at $s=2$, in which the dominance passes from the lower to the upper bound of the integral in Eq. (4.6) (recall $x_c \propto 1/T$). Above this crossover the final temperature dependence is independent of the parameters (i.e., T^2 in each case) and corresponds to that of the usual Fermi liquid model. Below the crossover the exponent depends on the particular property being considered but is always below that normally associated with a Fermi liquid state. We see that non-Fermi-liquid exponents are favored for small d and large l, i.e., in reduced dimensions or at the critical point where $\chi^{-1} \rightarrow 0$ as $T \rightarrow 0$.

In arriving at the leading temperature dependences given above, we have assumed $\Gamma_{\boldsymbol{q}}$ to be independent of T. In the critical case where $T_c \rightarrow 0$, this assumption is valid only if χ^{-1} in $\Gamma_{\boldsymbol{q}}$, as given in Eq. (4.2), is ignorable compared with $cq_{\hat{T}}^2$, where $q_{\hat{T}}$ is a typical thermal wave vector defined by $k_B T \sim \hbar\Gamma q_{\hat{T}}$ (so that $T \propto q_{\hat{T}}^z$). The equivalent condition that the correlation wave vector $\kappa = \sqrt{1/c\chi}$ be much smaller than $q_{\hat{T}}$ at low T is satisfied if the effective dimension of the problem, $d+z$, exceeds 4. The latter result follows directly from $q_{\hat{T}} \propto T^{1/z}$ and the expression for the temperature-dependent part of the inverse susceptibility $\Delta\chi^{-1}$ given in Sec. IV F below. There it will be shown that $\Delta\chi^{-1}$ is of the form in Eq. (4.7) with $m=n$, so that in leading order $\Delta\chi^{-1} \propto T^{(d+n)/z}$. In order that $\Delta\chi^{-1} \ll cq_{\hat{T}}^2$ as $T \rightarrow 0$ we need $d+n>2$ which is satisfied if $d+z>4$ since $z=n+2$.

D. Resistivity

The electrical resistivity $\Delta\rho$ due to the scattering of fermions from the exchange field, i.e., from spin fluctuations, is normally described in the Born approximation via the Boltzmann transport equation. In terms of the population function $n_{\boldsymbol{q}}$ introduced in Eq. (4.4), the conventional expression[5] for $\Delta\rho$ can be recast into the form[3]

$$\Delta\rho = \zeta \sum_{q<q_c} q^k \left(T \frac{\partial n_{\boldsymbol{q}}}{\partial T} \right)_\Gamma, \tag{4.8}$$

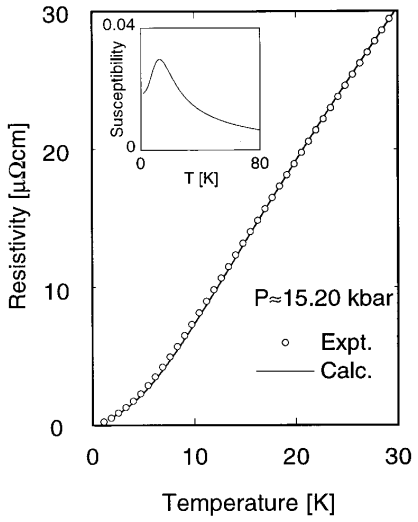

FIG. 8. Comparision of measured (○) and calculated (solid line) temperature dependence of the resistivity $(\rho-\rho_0)$ near p_c. The calculation is based on the model in the text, Eq. (4.2), with χ vs T from bulk measurements (inset in SI units), γ and c from inelastic neutron scattering measurements in zero pressure (Ref. 4), and a wave vector cutoff equal to the Brillouin zone dimension (ΓX). The vertical scaling factor [ζ in Eq. (4.8)] is the only free parameter in the comparison.

where ζ is a coupling parameter (independent of T in the Born approximation), and the subscript Γ implies a derivative at constant $\Gamma_{\boldsymbol{q}}$ in Eq. (4.4) and for the problem of interest here we expect $k=2$. The q^2 factor reflects the role of backscattering, i.e., the fact that high-q fluctuations are more effective than those at low q in reducing the current. Normally $(T\partial n_{\boldsymbol{q}}/\partial T)_\Gamma$ and $n_{\boldsymbol{q}}$ have the same leading-order dependence on T, and so to leading order the dependence of $\Delta\rho$ on T is given by Eq. (4.7) with $m=2$.

From Eq. (4.7) we predict $\Delta\rho\propto T^2$ when $(d+2)/l>2$. As expected this includes the case of a normal Fermi liquid with nonsingular interactions (in which $n=l=1$). In the critical region where $l=z$ we have $\Delta\rho\propto T^\beta$ with $\beta=(d+2)/z$, provided that $1<\beta<2$ and $d+z>4$. Thus with $z=3$ we find $\beta=\frac{5}{3}$ in three dimensions[22] and $\beta=\frac{4}{3}$ in two dimensions.[8,9] Note that in both these cases the effective dimension $d+z$ is indeed greater than 4.

The value of β (i.e., $\frac{5}{3}$) obtained with $d=z=3$ agrees well with the asymptotic low-temperature form of $\Delta\rho$ observed in MnSi. A detailed comparison of the predictions of the model contained in Eqs. (4.1)–(4.4), and (4.8) with experiment is presented in Fig. 8. Our numerical analysis of $\Delta\rho$ is based on the model for $\Gamma_{\boldsymbol{q}}$ given in Eq. (4.2) with $\chi^{-1}(T)$ taken from experiment at p_c and the fixed parameters γ and c inferred from inelastic neutron scattering data at zero pressure.[4] The cutoff q_c in the $\boldsymbol{q}$-space sum has been taken to be the Brillouin zone dimension π/a where $a=4.56$ Å, and ζ, the only free parameter, was chosen to allow comparison of the predicted and measured temperature dependence of ρ. It is significant that the model accounts not only for the non-Fermi-liquid exponent β at low T, but also quantitatively for the observed crossover to an intermediate quasilinear temperature variation of ρ at high T.

Our expression for ρ given in Eq. (4.8) assumes that the molecular field $\lambda_{\boldsymbol{q}}$, connecting $\boldsymbol{m}_{\boldsymbol{q}}(t)$ to the corresponding component of the molecular field, is essentially independent of $\boldsymbol{q}$ below a suitably defined cutoff wave vector q_c. Note, however, that the singular component of $\Delta\rho/T^2$ near p_c is not sensitive to this cutoff. The derivation of the standard model for $\Delta\rho$, on which Eq. (4.8) is based, implicitly assumes that transitions brought about by the scattering with the molecular field are indeed effective in reducing the *total* current. In MnSi justification for this assumption is provided by the large number of scattering channels offered by its open, multisheet Fermi surface.[11,15]

We also note that since χ^{-1} in MnSi does not strictly vanish at low T even near p_c (see Sec. III), we may expect $\rho\propto T^2$ at sufficiently low T for all p. Our numerical analysis, however, suggests that this limiting form should only be clearly observable for $p>p_c$ at temperatures well below the presently accessible experimental range.

E. Heat capacity

Further insights into the nature of the state in which $d=z=3$ as described by the above may be gained by considering (i) the quasiparticle scattering rate, which is related to Eq. (4.8), but *without* the backscattering weighting factor q^2, and (ii) the quasiparticle effective mass defined via the electronic heat capacity divided by T. Note that throughout this paper quasiparticle properties are assumed to be defined as suitable averages near the Fermi energy.

The correction ΔC to the total heat capacity arising from the effects of the exchange field may be obtained from the thermodynamics of this field treated as a collection of coupled modes. In a mean-field approximation for the mode-mode coupling,[5–7] we arrive at an expression for ΔC, which, in terms of the population $n_{\boldsymbol{q}}$ of Eq. (4.4), reduces to the elementary form[3]

$$\Delta C\simeq\frac{3\hbar}{2}\sum_{q<q_c}\Gamma_{\boldsymbol{q}}\frac{\partial n_{\boldsymbol{q}}}{\partial T}. \tag{4.9}$$

In writing this we suppose that our system is in the limit where many-body effects are dominant. In particular we are assuming that $\Gamma_{\boldsymbol{q}}$ is strongly suppressed below the behavior expected in the absence of the effects of the molecular field or, precisely, that $\lambda_{\boldsymbol{q}}=\lambda_{\boldsymbol{q}}\chi^0_{\boldsymbol{q}}$ is of order unity for $q<q_c$, where $\chi^0_{\boldsymbol{q}}$ is $\chi_{\boldsymbol{q}}$, but in the absence of the enhancement produced by the exchange field. The wave vector dependence of $\lambda_{\boldsymbol{q}}$ can be crudely described via the choice of cutoff wave vector q_c, the magnitude of which does not in practice greatly effect the singular part of ΔC near the quantum critical point. We also comment that the factor of $\frac{3}{2}$ in Eq. (4.9) arises from our choice in Eq. (4.4) of definition for $n_{\boldsymbol{q}}$. The factor of 3 reflects the number of Cartesian components of $\boldsymbol{m}_{\boldsymbol{q}}$ for each $\boldsymbol{q}$, and the factor of $\frac{1}{2}$ highlights the fact that the mean energy of an overdamped mode has a *potential* but no *kinetic* component. We note that for undamped modes with spectrum $\Omega_{\boldsymbol{q}}$ and a degeneracy of 3 for each $\boldsymbol{q}$, the heat capacity is given by Eq. (4.9) with $\Gamma_{\boldsymbol{q}}/2$ replaced by $\Omega_{\boldsymbol{q}}$ and $n_{\boldsymbol{q}}$ replaced by the Bose factor n_ω evaluated at $\omega=\Omega_{\boldsymbol{q}}$. In the high-$T$ limit, the latter yields a heat capacity per mode which is, as expected, twice that given by Eq. (4.9) (provided the temperature dependence of $\Omega_{\boldsymbol{q}}$ and $\Gamma_{\boldsymbol{q}}$ can be ignored).

To leading order in T, ΔC is given by Eq. (4.7) with $m=l$ all divided by a factor of T so that

$$\Delta C \propto \begin{cases} T^{d/l}, & d<l, \\ T\ \ln(T^*/T), & d=l\ , \\ T, & d>l, \end{cases} \tag{4.10}$$

where T^* is a constant. The case in which $d>l$ covers the usual Fermi liquid description (where $d=3$ and $l=n=1$) and as expected gives ΔC to be linear in T. For MnSi in which $p\sim p_c$ we have $d=3$ and $l\rightarrow z=3$ and so the case with $d=l$ applies.

In cases such as MnSi with $p\sim p_c$, the result for ΔC and a corresponding analysis of the quasiparticle scattering rate yield expressions for the effective *mass* and *cross section* having the singular forms $\ln(T^*/T)$ and $1/T$, respectively. In this limit, where the *mass* diverges logarithmically, the relative probability that a quasiparticle state is equivalent to a bare particle state with the same wave vector on the Fermi surface vanishes logarithmically as $T\rightarrow 0$. Since the logarithm is a minimal singularity, the conventional Fermi liquid may be said to be just at its limit of applicability. The above singular forms for the *cross section* and *mass* define the state called a *marginal Fermi liquid*.

Similar forms for the quasiparticle *cross section* and *mass* have been obtained by another approach in the case of the long-range Lorentz magnetic force,[2] for which we also have $d=z=3$. A quantitative analysis, however, suggests that the singular effects of this interaction, which is characterized by a very stiff spectrum $\Gamma_{\boldsymbol{q}}$, would be difficult to detect experimentally. A different type of marginal state has also been introduced and extensively developed in connection with the nonsuperconducting phases of some of the copper oxide systems (see, e.g., Ref. 23).

Note that in lower dimensions, the singularities in the quasiparticle properties become stronger than marginal. In particular for $d=2$ and $z=3$ the above analysis leads to a *mass* which in the low-temperature limit diverges as $T^{-1/3}$. This is consistent with results obtained in Refs. 8 and 9 for a model having the same values for d and z but in which the relevant molecular field is associated not with the magnetization, but with a chiral field related to third-order nonlocal products of the magnetization.

Analyses based on the language of quantum critical phenomena (see, e.g., Refs. 3, 20 and 21) as well as more recent studies based on a diagrammatic evaluation of the self-energy of fermions interacting with suitably defined molecular fields[8,9,24] suggest that the above models for the quasiparticle *cross section* and *mass* yield the correct singular temperature-dependent terms at the quantum critical point, provided the effective dimension $d+z$ exceeds the upper critical value of 4, a condition that is satisfied in both the cases (i.e., with $d=z=3$ or when $d=2$ and $z=3$) mentioned above.

For comparison, we now consider briefly the case in which the critical fluctuations are not centered on $\boldsymbol{q}\rightarrow 0$, but around some antiferromagnetic wave vector $\boldsymbol{Q}$ of the order of the dimension of the Brillouin zone. In this case, it is useful to change the origin by replacing $\boldsymbol{q}$ by $\boldsymbol{Q}+\boldsymbol{q}$. To lowest order in q, $\Gamma_{\boldsymbol{Q}+\boldsymbol{q}}=\gamma_{\boldsymbol{Q}}(\chi_{\boldsymbol{Q}}^{-1}+cq^2)$, where $\gamma_{\boldsymbol{Q}}$ is a nonvanishing constant.[5] The exponent n is now effectively 0 rather than 1. In the limit as $\chi_{\boldsymbol{Q}}^{-1}\rightarrow 0$, we obtain $\Gamma_{\boldsymbol{Q}+\boldsymbol{q}}\propto q^2$ and hence a dynamical exponent z of 2 rather than 3. The difference arises from the Landau damping factor in the relaxation rate, which vanishes as the first power of the wave vector around the origin in the Brillouin zone of a homogeneous system. When the effective dimension $d+z$ is greater than 4 the heat capacity is again expected to be described by Eq. (4.9). For $d=3$ and $z=2$ this condition is satisfied, and we find that $\Delta C/T$, while not strictly singular[5] as $T\rightarrow 0$, can nevertheless display a strong and anomalous increase with decreasing T. Moreover, the variation with temperature is qualitatively similar to that found in the marginal case discussed earlier.

We note that the true marginal case as described above requires $d=z$ and so in a case with $z=2$ the effective dimension $(d+z)$ does *not* exceed the upper critical value of 4 that is strictly required for a simple description. We also comment that for antiferromagnetic fluctuations, the standard analysis for the resistivity, in contrast to that for the heat capacity, may not be strictly applicable even when the condition $d+z>4$ is satisfied.[25]

F. Magnetic susceptibility

Finally we present a brief discussion of the temperature dependence of χ and of the pressure dependence of T_c. In the mean-field approximation for the mode-mode coupling,[5,6] the temperature dependence of χ^{-1} can be expressed in terms of the population function $n_{\boldsymbol{q}}$ defined in Eq. (4.4) as

$$\Delta\chi^{-1}=5b\sum_{q<q_c}^{\wedge}\gamma_{\boldsymbol{q}}n_{\boldsymbol{q}}, \tag{4.11}$$

where b is the anharmonicity coefficient, $\hat{\Sigma}$ denotes a sum per unit volume, and $\gamma_{\boldsymbol{q}}$ is defined in Eq. (4.2). In the simplest case, b is the coefficient of the cubic term in an expansion of the magnetic equation of state $H(M)=aM+bM^3$ at $T=0$, where in equilibrium $H(M)$ is the uniform magnetic field which stabilizes the bulk magnetization M.

The expression in Eq. (4.11) for $\Delta\chi^{-1}$ is of the form in Eq. (4.7) with the exponent m equal to n. It follows that when $l\rightarrow z=2+n$, $\Delta\chi^{-1}\propto T^{(d+n)/z}$, provided $z<(d+n)<2z$ and $d+z>4$. If we write $\chi^{-1}=a+\Delta\chi^{-1}$ and expand the $T=0$ limit of χ^{-1} around p_c as $a\propto(p-p_c)$, the condition $\chi^{-1}(T_c)=0$, defining T_c, yields $T_c^{(d+n)/z}\propto(p_c-p)$. Thus for $d=3$ we have $T_c^{4/3}\propto(p_c-p)$ for $n=1$ $(z=3)$ and $T_c^{3/2}\propto(p_c-p)$ for $n=0$ $(z=2)$, i.e., for the ferromagnetic and antiferromagnetic cases, respectively. These results for the pressure dependence of T_c are based on a mean-field treatment analogous to the classical Landau model of second-order phase transitions, which may be expected to hold when the appropriate dimension $(d+z)$ exceeds the upper critical dimension of 4 (see Refs. 3, 20 and 21).

For MnSi this description is incomplete since the coefficient b of the M^3 term in H vs M is believed to be *negative* at low T. For stability, a minimal description must therefore include terms in H vs M up to at *least fifth* order in M. If a fifth-order description is sufficient, a straightforward extension of the mean-field approximation leads to a shift in the coefficient of the cubic term in $H(M)$ of

$$\Delta b = 14g \sum_{q<q_c}^{\wedge} \gamma_q n_q \tag{4.12}$$

and to a replacement of b in Eq. (4.11) by $(b+\Delta b/2)$. Here g is the coefficient (assumed positive) of the M^5 term in H vs M. A model of this kind provides the basis of a detailed account, to be discussed more fully elsewhere, of the form of χ^{-1} vs T and p. In particular, the latter correctly describes (i) the crossover at p^* from a transition of second order to one of first order, (ii) the peak in χ vs T in the paramagnetic state, and (iii) the overall pressure dependence of T_c. This analysis also shows that the $T_c^2 \propto (p_c - p)$ form observed in the range $p^* < p < p_c$ arises from the fact that, in this first-order regime, an abrupt jump occurs from a marginal Fermi liquid state above T_c to a (partly) spin-polarized Fermi liquid state below T_c. In particular, this form of T_c vs p does not imply a simple Fermi liquid description of the paramagnetic state. We also note that the $T_c^{4/3} \propto (p_c - p)$ pressure dependence of T_c, predicted by the simplest model for $\Delta\chi^{-1}$ when $d=z=3$, is indeed observed in the low-temperature ferromagnet $ZrZn_2$, which, unlike MnSi, shows no evidence for a first-order transition near the critical pressure.[26]

V. FURTHER DISCUSSIONS

The considerations of Sec. IV F do not alter our theoretical description of ρ vs T as given in Sec IV B since that was based on the *measured* form of χ^{-1} vs T (Fig. 6) and not on that expected for the simple model in Eq. (4.11) in which the anharmonicity parameter is assumed to be positive at low T. Although small, χ^{-1} does not actually vanish as $T \to 0$ at p_c, and hence for sufficiently low T, ρ is expected to enter a T^2 regime in an ideally pure sample. The tiny magnitude of χ^{-1} (typically 10^3 times lower than that in normal metals) and the q^2 factor favoring large-q fluctuations in the sum in Eq. (4.8) mean that this crossover to Fermi liquid behavior is only expected to occur in the low-mK range where, in practice, other effects such as impurity scattering begin to dominate.

Numerical analyses based on Eqs. (4.1)–(4.4) and (4.8) also suggest that a recovery of a Fermi liquid form for ρ above 1 K will take place only at relatively high pressures, i.e., several times p_c. Thus, the range in p over which a description in terms of a marginal Fermi liquid model is useful can be wider than might be naively supposed. This should be contrasted with the rapid return to a T^2 form of ρ found below T_c (Fig. 3) or in an applied magnetic field.[27] The rapid recovery of the Fermi liquid form in these cases arises from the strong attenuation of the spin fluctuation amplitude resulting from suppression of transverse and stiffening of longitudinal components in the presence of a uniform spin polarization.

Our aim has been to present a plausible minimal interpretation of the main features of the resistivity and susceptibility data. A number of more subtle effects should also be considered in a more complete analysis. These would include corrections due to (i) a small relativistic term in the local free energy arising in structures lacking inversion symmetry (e.g., $B20$ for MnSi), (ii) nonlinear precession of the magnetization under the action of the molecular field, (iii) screening of the mode-mode coupling parameters (b and g), and (iv) the magnetovolume effect.

The lack of inversion symmetry, together with the (albeit weak) spin-orbit interaction (i), leads to the appearance of critical fluctuations around a small but finite wave vector of magnitude $Q \simeq 0.033$ Å^{-1},[4,10] as well as to a very weak first-order magnetic transition even below p^*.[28] We note, however, that the typical thermal wave vector $q_{\hat{T}}$ defined by $\hbar\Gamma_{q_{\hat{T}}} \sim k_B T$ is at least an order of magnitude greater than Q for $T \geqslant 1$ K. Thus, any corrections to the results of Sec. IV D are expected to be small, except at extremely low temperatures near p_c. (We also note that for typical values of $q_{\hat{T}}$ in our experimental range, thermal magnetic fluctuations can link different sheets of the multiply connected and open Fermi surface of MnSi and therefore facilitate transfer of momentum away from the electron system.)

The effects of nonlinear precession (ii) and screening beyond the Hartree approximation (iii) have also been considered.[3] The latter leads to qualitative changes only in the Ginzburg regime, which collapses as $T_c \to 0$ for an effective dimension $d+z$ greater than 4. Both (ii) and (iii) are important quantitatively in the region of crossover from a second- to a first-order transition, and more generally can lead to different renormalizations of the parameter b entering the temperature dependence of the susceptibility given by Eq. (4.11) and the magnetic equation of state. Since our analysis of the resistivity was based on the observed $\chi(T)$, it is unaffected by these considerations.

The magnetovolume effect (iv) leads to further renormalization of the parameters of the model and can, in principle, effectively lead to a negative value of the anharmonicity parameter b, and so to a first-order transition near p_c. However, it is interesting to note that a value for b, consistent with observation in sign and order of magnitude, can already be obtained in a single-particle analysis based solely on the band-calculated density of states which has a deep minimum at the Fermi level.[11,29]

In summary, we find that the above corrections are either small and ignorable in our experimental range, or can be absorbed into the parameters of the model [$\chi(T)$, c, and γ], which are empirically determined. Furthermore, the deep minimum of the one-particle density of states at the Fermi level appears to be sufficient on its own to account for the sign and strength of the mode coupling parameter required for a description Sec. (IV F) of the crossover from a *second-* to weakly *first-* order transition near p_c.

VI. CONCLUSION

In conclusion, we find that near and above p_c the behavior of MnSi is consistent with a model of a marginal Fermi liquid in which a long-range effective interaction between quasiparticles arises via the exchange of long-wavelength nearly critical fluctuations in the spin density. The applicability of an elementary treatment of such fluctuations may be connected with the fact that the effective dimension $d+z$, appropriate to critical phenomena in the *quantum* limit, is

above the upper critical value of 4 (i.e., the Ginzburg regime, where corrections to a mean-field description are important, becomes vanishingly small). The description of ρ in terms of a marginal Fermi liquid model is expected to fail at very low T due to the occurrence of a (weak) first-order transition near p_c, which implies that χ (though exceptionally enhanced) remains finite as $T \to 0$, $p \to p_c$. The range of applicability of the non-Fermi-liquid form of ρ may extend over an even greater range in a related ferromagnet $ZrZn_2$ in which a first-order transition appears to be absent near p_c and above at least 0.9 K.[26]

ACKNOWLEDGMENTS

We wish to thank N. R. Bernhoeft, P. Coleman, J. Flouquet, M. Grosche, D. Khmelnitskii, A. Millis, E. Papavasiloupolos, S. Sachdev, and A. Tsvelik for informative discussions. The highest-purity specimen used in this study was prepared for an earlier study of the de Haas–van Alphen effect in collaboration with L. Taillefer.[11] This research has been supported both by the EPSRC of the UK and the EU.

[*]Present address: Physikalisches Institut, Universität Karlsruhe, 76128 Karlsruhe, Germany.

[1] P. W. Anderson (unpublished).

[2] T. Holstein, R. E. Norton, and P. Pincus, Phys. Rev. B **8**, 2649 (1973); M. Reizer, *ibid.* **39**, 1602 (1989).

[3] G. G. Lonzarich, in *The Electron*, edited by M. Springford (Cambridge University Press, Cambridge, England, 1996) and references therein; and (unpublished).

[4] Y. Ishikawa, Y. Noda, Y. J. Uemura, C. F. Majhrzah, and G. Shirane, Phys. Rev. B **31**, 5884 (1985); S. A. Brown, N. R. Bernhoeft, S. H. Hayden, and G. G. Lonzarich (unpublished); see also Ref. 15; P. Harris, B. Lebech, H. S. Sim, K. Mortensen, and J. S. Pedersen, Physica B **213&214**, 375 (1995); S. A. Sorensen and B. Lebech (unpublished).

[5] T. Moriya, *Spin Fluctuations in Itinerant Electron Magnetism* (Springer, Berlin, 1985) and references therein.

[6] G. G. Lonzarich, J. Magn. Magn. Mater. **45**, 43 (1984); **54-57**, 612 (1986); G. G. Lonzarich and L. Taillefer, J. Phys. C **18**, 4339 (1985), and references therein.

[7] G. J. McMullan, Ph.D. thesis, University of Cambridge, 1989.

[8] See, e.g., P. A. Lee and N. Nagaosa, Phys. Rev. B **46**, 5621 (1992).

[9] See, e.g., B. L. Altshuler, L. B. Yoffe, and A. J. Millis, Phys. Rev. B **50**, 14 048 (1994).

[10] Small-angle neutron scattering experiments performed at Saclay confirm the presence at zero field of a helical modulation of $2\pi/Q \simeq 190$ Å along $\langle 111 \rangle$ in the highest-purity specimen investigated here.

[11] L. Taillefer, G. G. Lonzarich, and P. Strange, J. Magn. Magn. Mater. **54-57**, 957 (1986).

[12] Y. Takahashi and T. Moriya, J. Phys. Soc. Jpn. **54**, 1592 (1985).

[13] J. D. Thompson, Z. Fisk, and G. G. Lonzarich, Physica B **161**, 317 (1989).

[14] C. Pfleiderer, G. J. McMullan, and G. G. Lonzarich, Physica B **206&207**, 847 (1995); **199&200**, 634 (1994); C. Pfleiderer, R. J. Friend, G. G. Lonzarich, N. R. Bernhoeft, and J. Flouquet, Int. J. Mod. Phys. B **7**, 887 (1993).

[15] S. A. Brown, Ph.D. thesis, University of Cambridge, 1990.

[16] I. R. Marsden, Ph.D. thesis, University of Cambridge, 1992.

[17] C. Pfleiderer, Ph.D. thesis, University of Cambridge, 1994; Rev. Sci. Instrum. (to be published).

[18] C. Pfleiderer, C. Thessieu, A. N. Stepanov, M. Couach, G. Lapertot, and J. Flouquet, Physica B (to be published).

[19] N. R. Bernhoeft, S. M. Hayden, G. G. Lonzarich, D. McK. Paul, and E. J. Lindley, Phys. Rev. Lett. **62**, 657 (1989); G. G. Lonzarich, N. R. Bernhoeft, and D. McK. Paul, Physica B **156&157**, 699 (1989).

[20] J. Hertz, Phys. Rev. B **14**, 1165 (1976).

[21] A. J. Millis, Phys. Rev. B **48**, 7183 (1993).

[22] J. Mathon, Proc. R. Soc. London, Ser. A **306**, 355 (1968).

[23] C. M. Varma, P. B. Littlewood, S. Schmitt-Rink, E. Abrahams, and A. Ruckenstein, Phys. Rev. Lett. **63**, 1996 (1989).

[24] D. Khmelnitskii and E. Papavasiloupolos (unpublished).

[25] R. Hlubina and T. M. Rice, Phys. Rev. B **51**, 9253 (1995).

[26] F. M. Grosche, C. Pfleiderer, G. J. McMullan, G. G. Lonzarich, and N. R. Bernhoeft, Physica B **206&207**, 20 (1995).

[27] C. Thessieu, A. N. Stepanov, G. Lapertot, and J. Flouquet, Solid State Commun. **95**, 707 (1995).

[28] P. Bak and M. H. Jensen, J. Phys. C **13**, L881 (1980).

[29] G. J. McMullan (unpublished).